

ADDRESSING THE NEEDS OF COMPLEX MEMS DESIGN

J.V. Clark¹, D. Bindel², W. Kao², E. Zhu², A. Kuo⁶, N. Zhou⁴, J. Nie²,
J. Demmel², Z. Bai⁵, S. Govindjee³, K.S.J. Pister², M. Gu², A. Agolino⁴

¹Applied Science & Technology, ²Electrical Engineering & Computer Science,

³Civil Engineering, ⁴Mechanical Engineering, ¹⁻⁴University of California at Berkeley, USA

⁵Computer Science, University of California at Davis, USA

⁶Electrical Engineering, University of Michigan, USA

ABSTRACT

In this paper, we report several advances in the Sugar2.0 MEMS system simulation package, including reduced-order modeling techniques, simple hierarchical description of complex structures, synthesis tools, a variety of models, and a web-based interface. Examples include the modeling of a torsional micromirror with lateral actuators compared to experiment, and the prototyping of a microrobot.

1 INTRODUCTION

Microelectromechanical systems are moving from the simple single-function devices of the past to more elaborate systems with complex structural intricacies with rich dynamic subtleties. However, despite the relatively large number of CAD for MEMS tools, products, and vendors, MEMS design today still largely consists of working at the whiteboard with colleagues and entering simplified equations into Mathcad, if not writing them by hand on the back of an envelope. Today's CAD tools are useful for design verification, but are not often used in the early phases of design. Additionally they are generally useful for in-depth simulation of an individual device fabricated in a new process, rather than a collection of devices forming an entire microsystem. Sugar [1] was created to investigate remedies to the above problems. Its framework exploits the familiar open-code Matlab environment, which invites features and modifications from users.

We have previously shown that the number of equations that describe many MEMS designs can be greatly reduced using modified nodal analysis while still maintaining accuracy within fabrication limits [2-4]. Test cases included the warping of an ADXL05 accelerometer due to residual stress and strain gradients, process variation analysis where the possible displacement distributions and worst case scenarios were predicted, the transient response of a gyroscope in an accelerated frame, electrical currents induced by a multimode resonator, geometrical optimization of a thermal actuator, and nonlinear frequency response analysis to name a few. The test cases were compared to experiment, theory, and/or finite-element analysis. Where many needs of the designer are difficult to address with strict FEA-based systems, we present remedies to several CAD-for-MEMS problems.

2 LARGE SYSTEMS

The simulation of large micro systems is often unreachable for designers using FEA with less than a few gigabytes of memory, or too time consuming to be practical, taking days to complete. Days may be reduced to hours in converting FEA to macromodels [5], which transforms semi-compliant components to rigid bodies (e.g., comb drives, plates). But hours may still be too time consuming for the user who wants to quickly explore design possibilities. Alternatively, the simulation may need to be embedded in a design computation that may require thousands of iterations, such as those required for optimization and evolutionary synthesis [10].

Sugar uses parameterized subnets for device components. These components are composed of physical modeling functions such as beams, electrostatic gaps, etc. User-definable model functions and subnets greatly expand Sugar's modeling capabilities and ease of design. This design methodology allows large and complex systems to be created quite easily. For example, the torsional micromirror in *Fig 1* consists of 2,621 elements and 11,706 spatial degrees of freedom. For FEA, this micromirror may consist of about a million nodes and over three million elements using an intermediate mesh refinement. The Sugar components that make up the device include perforated torsional beams, comb drive arrays, torsional springs assemblies, a circular plate, and cosine-shaped beams. Combining these components into a complete system only requires eleven lines of netlist text. Input parameters may be used to modify material property and geometry, such as Young's modulus, beam widths, number of comb arrays, diameter of the mirror, number of holes in perforated beams, etc. Conversely, other CAD packages may require hours to modify such designs.

An SEM of the micromirror is provided in *Fig 2*, which shows the complexity of the perforated torsional beams, extended moment arms, and the three structural layers. A view from underneath, *Fig 3*, shows how Sugar faithfully reproduces the structural layers. The function of the 3-layer process is to 1) reduce the mass of the mirror, and 2) produce a moment arm on the mirror.

Sugar simulation versus experimental data [6] is shown in *Fig 4*. *Fig 5* shows a multidimensional plot where mirror tilt is plotted against sweeping both the moment arm lengths and the perforated beam widths with respect to a constant voltage.

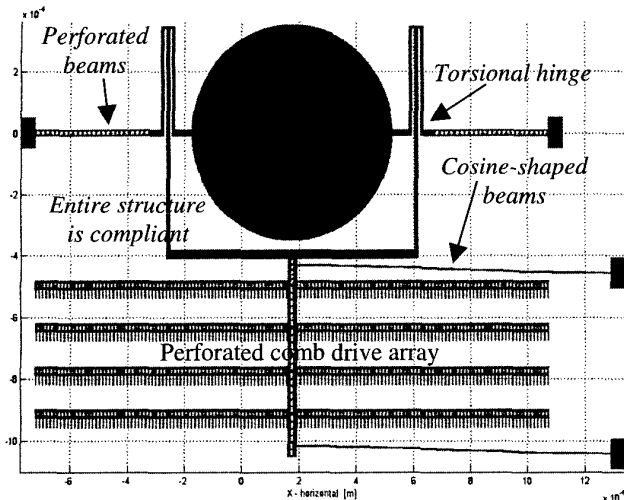


Fig 1: Torsional micromirror. 11,706 spatial degrees of freedom. The perforation of beams increases lateral stiffness while reducing torsional stiffness. The reduced mass of the perforated comb drive increases resonance frequency. The cosine-shaped beams minimize the comb drive's transverse displacement. Equivalent nodal forces and moments are calculated from the distributed load due to each comb finger.

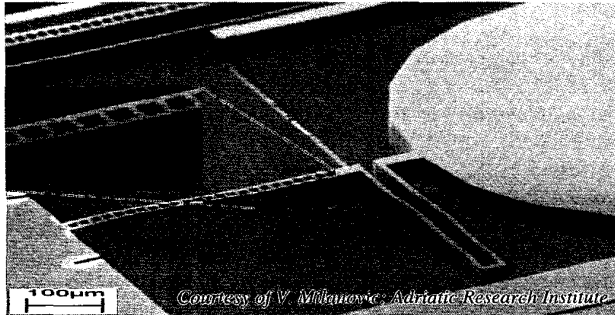


Fig 2: SEM [6] of the torsional hinge. The insert shows an enlarged view of the perforated beam.

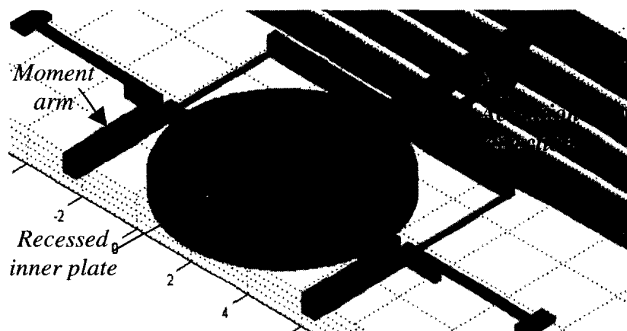


Fig 3: A view from underneath shows the rim of the mirror, which raises the mirror's center of mass. The lower mass increases resonance frequency. The mass of the circular mirror is about twice the mass of the perforated comb drive array.

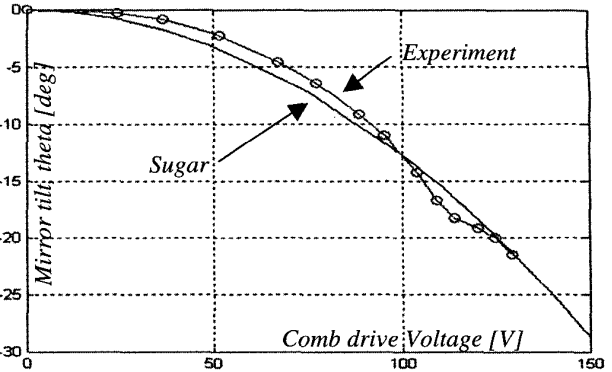


Fig 4: Sugar vs experiment of the system in Fig 2.

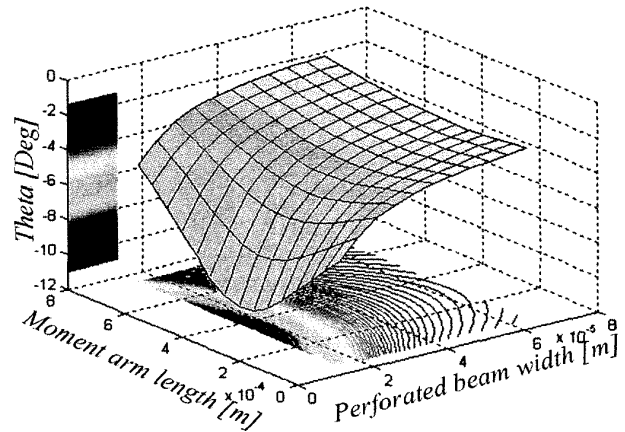


Fig 5: Surface and contour plot of theta (mirror tilt), vs perforated beam width, vs moment arm length, for an 80V actuation

3 SYNTHESIS TOOLS

Most MEMS tools are borrowed from the electronics industry. The available layout tools are typically geared toward the circuit designer, leaving the MEMS designer the arduous task of creating MEMS-related features for large systems such as etch holes and geometrically varied test-arrays, which are time consuming, prone to errors, and not easily modifiable.

Sugar2.0 now features the industry standard CIF export for rectangular geometries. Therefore designs characterized in Sugar can go straight to fab or be exported into an FEA CAD for MEMS package for critical fine-tuning. To complete the I/O layout loop, CMU collaborators [7] have developed a CIF extractor which converts a CIF file into a Sugar netlist.

Etch holes are often necessary for the release of wide structures. Large complex layouts may need thousands of such holes strategically placed. The user performs this tedious task by adding holes when the design rule checker algorithm complains. Sugar makes this process systematic by automatically generating etch holes where needed. This may also aid performance yield for particular designs since etch holes affect mass, damping, and stiffness. Dimensions and

spacing between etch holes may be edited as well. Fig 6 shows Sugar's CIF output of a folded flexure loaded into Cadence. Both the etch holes and anchors-connects were automatically generated.

Another important issue for the MEMS designer is material characterization such as Young's modulus, stress, and slight changes in geometry from layout. The data is usually obtained by creating geometrically varied arrays of a test device such that material properties may be extracted from the varied dependencies. Fig 7 shows an array of gap-closing actuators, where orientation, proof-mass width, and cantilever length were swept. Generating a test array in Sugar simply involves a nested for-loop. Here, the electrical connection is conveniently lengthened during rotation so that the bonding pads remain positioned for ease of automated probe testing.

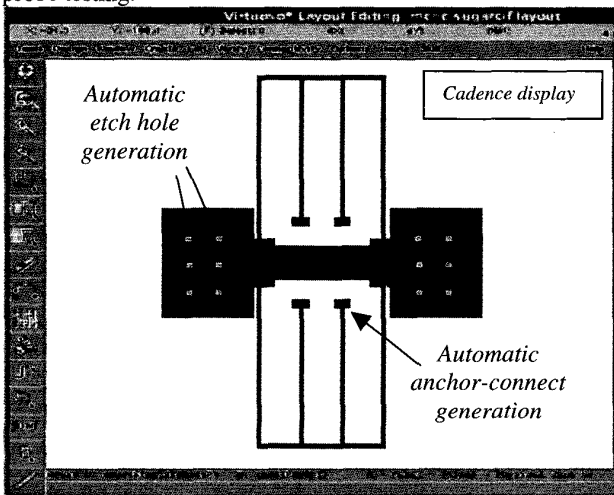


Fig 6: The CIF output of Sugar in Cadence. Sugar automatically puts in etch-holes and anchor-connects, which saves a lot of time for large, complex layouts.

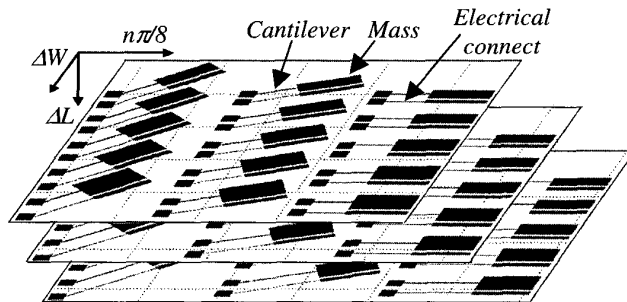


Fig 7: Array generation of a gap-closing actuator for material characterization. Orientation, vs cantilever length, vs proof-mass width.

4 NONLINEAR ELEMENTS

FEA is commonly used to model large deflections of beams since node-based models are usually only valid over small deflections. Our single-element two-node model agrees well with large-deflection theory for thin beams [8].

We use a piece-wise continuous 3rd-order polynomial of the form $F=K_{Lin}q+K_{NonLin,i}q^3$, where K_{Lin} is linear stiffness matrix, $K_{NonLin,i}$ are the cubic nonlinearities, and the i index is a function of the displacement vector q . A complete derivation can be found at [1]. To see the significance of the nonlinear stiffness term, a simulation comparing deflections of a nonlinear beam against a linear beam is provided in Fig 8. Both cantilevers have the same geometry, material properties, and applied forces. A succession of five lateral forces F_Y demonstrates the growing inaccuracy of the linear model as lateral displacements increase.

For small displacements, lateral deflections for both models are similar. The nonlinear model begins to depart from the linear approximation when the lateral deflection to length ratio surpasses $\sim 20\%$. As F_Y increases, the nonlinear beam does not deflect as much as the linear beam due to the increased stiffening that's a function of displacement. Also note that the overall beam length is preserved in the nonlinear model; not so for elementary linear beam theory since the axial and lateral displacements are decoupled.

Force-deflection curves of Sugar's nonlinear beam model versus large deflection theory are shown in Fig 9. One way to read the graph is to first determine the magnitude of a nondimensional force defined as $F_Y L^2/EI$. The curves crossing this value are the corresponding axial, vertical, and rotational displacements of the cantilever's end node.

We're currently extending this particular nonlinear beam theory to model the deflection of beams with simultaneous lateral forces, axial forces, and moments. Using the principle of elastic similarity and the geometrical nature of elliptic integrals [9], we have formulated an analytical nonlinear multiple force-deflection relationship for cantilever beams [1]. The results are shown in Fig 10. Here, both lateral and axial forces are applied to a cantilever, while the resultant $|F_X+F_Y|$ remains constant. For $F_X=0$, the curves are identical to those in Fig 9. As F_X increases, the lateral, axial, and rotational displacements increase slightly, moderately, and significantly, respectively.

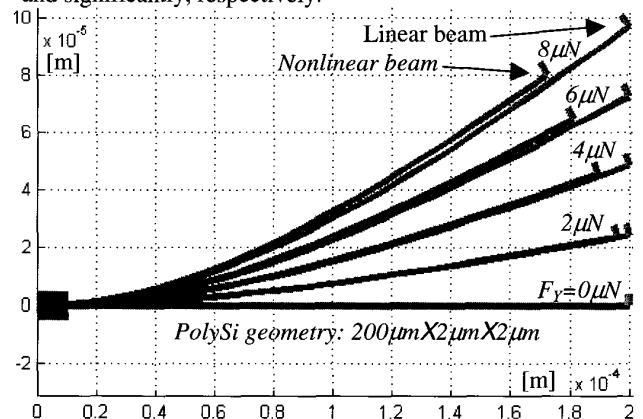


Fig 8: Nonlinear vs linear deflections. Superimposed pairs of cantilevers subjected to five vertical forces. The nonlinear beam experiences increased vertical stiffness in bending while preserving its overall length. Static analysis takes 0.04sec (0.01sec) for the nonlinear (linear) model on an Intel P4.

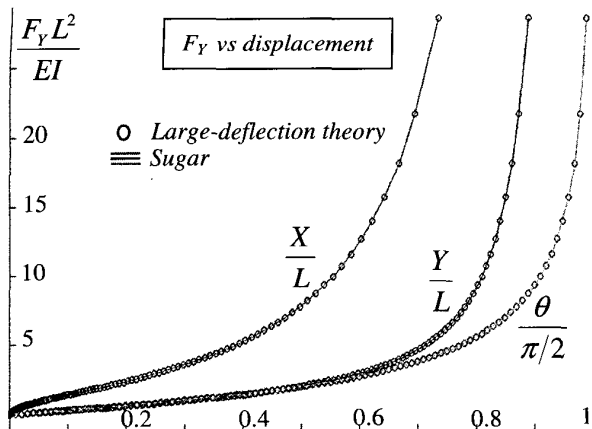


Fig 9: Sugar versus large-deflection theory [1]. Axes are generalized to nondimensional units. F_Y is a lateral force as applied in Fig 8.

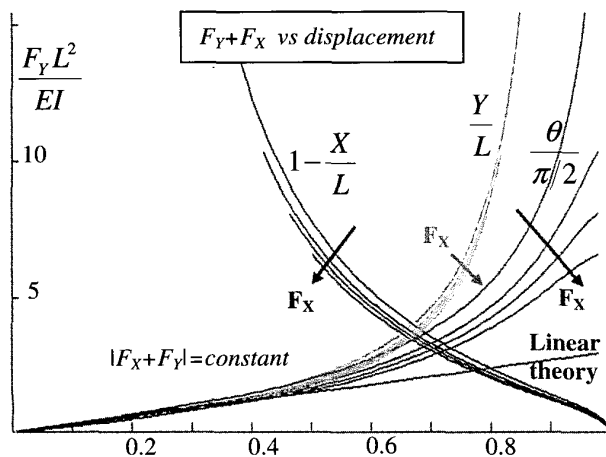


Fig 10: An analytical extension of the formulation shown in Fig 9 where an increasing axial force F_X is introduced. The resultant $|F_Y+F_X|$ remains constant. The straight line represents the lateral and rotational displacements for a linear beam, which are both independent of F_X .

5 COMPLEX SYSTEMS

MEMS design and dynamic analysis may be further complicated by the use of hinges, angled sliders, contact, and sliding friction. Hinges allow planar structures to deflect out of plane (e.g., corner-cube reflectors, scanners), and angled sliders may be used in large deflection actuation (e.g., inchworm motors). Though these kinds of components are often fabricated, they have not been readily utilized in standard CAD for MEMS packages. Fig 11 shows hinges, torsional hinges, and sliders used in prototyping a microrobot. BSAC students are using Sugar to explore the many issues involved in getting smart-dust to walk such as gravitational effects, parasitic electrostatic forces, maneuverability, work requirements.

The combined legs and tethers must withstand the compressive weight of the robot itself, on top of carrying any additional load. Under maximum load, the walking microrobot may need to keep as many as five legs in contact with the ground at any time. Placing the entire microsystem in an accelerating frame, through which the substrate is given an upward acceleration g , generates the equivalent gravitational forces upon each node. Maneuverability of the robot is also an important issue if it is to perform a task. The design shown in Fig 12 walks in a crab-like fashion where each two-degree of freedom leg may extend, lift, and contract. For now, we model foot-to-ground contact using microhinges, where a foot in contact may rotate but not translate. This limits walking analysis to one step back and forth, and slight turns. Sliders positioned on the torso of the robot actuate legs. External forces applied to the sliders pull on the microhinged tethers. These forces represent the minimum force requirement for an actual actuator such as an inchworm motor.

Future work in this area includes friction in the hinge and slider; discrete-time event simulation of multiple steps where foot-to-ground contact toggles on and off according to threshold guards; actuation motors; and robust designs.

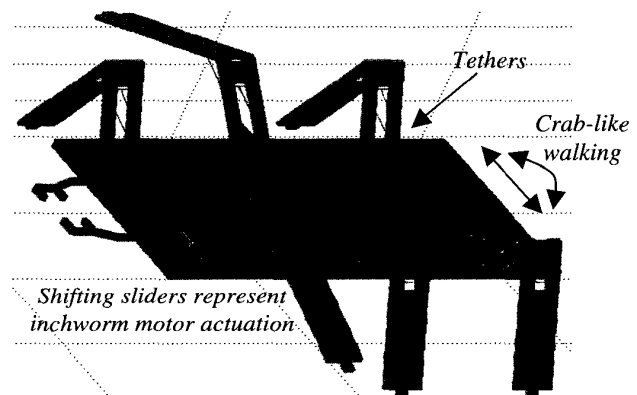


Fig 11: Microrobot prototype. Sliders actuate thigh and shin for crab-like maneuvering. Static solution of this 858-dof system takes seven seconds on an Intel P4.

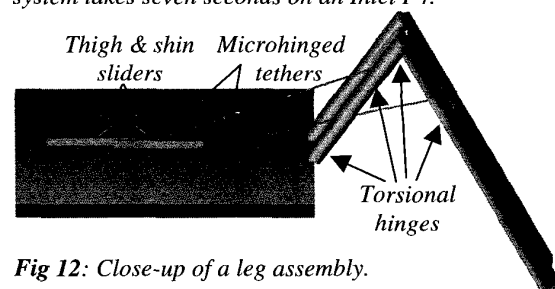


Fig 12: Close-up of a leg assembly.

6 REDUCED ORDER MODELING

The idea behind reduced-order modeling is to reduce the order p of the following frequency response function of the

microsystem

$$H_p(j\omega) = f_p^T (-\omega^2 M_p^2 + j\omega D_p + K_p)^{-1} f_p$$

where the size of the mass M_p , damping D_p and stiffness K_p matrices is $p \times p$, and ω is the excitation frequency. Traditionally, the above second-order frequency response function is first linearized before applying a reduced-order modeling technique to obtain a reduced-order model. By this approach, the reduced-order model stays in linear form, and cannot be represented in the second-order form.

We report that we have developed a new Krylov subspace technique, which results in a reduced-order model in the desired second-order form. The approach is based on an early work by Su and Craig Jr. [11] and on recent progress in the research of Krylov subspace techniques for reduced-order modeling. There are a number of advantages for such approach in terms of preserving symmetry, stability and physical meaning of the original system. Furthermore, the reduced-order model can also be used for other analysis and synthesis of the original system.

Applying these reduced-order techniques to the 11,706-order micromirror from section 2 (LARGE SYSTEMS), we find that a reduced-order model of order $p=20$ is sufficient for excitation frequencies in the range 0-5 kHz. For higher frequencies, 5-10 kHz, $p=40$ is sufficient for desired accuracy. Bode and phase plots of the micromirror are shown in Fig 13-14, where the reduced-order frequency response function $H_{40}(j\omega)$ is superimposed upon the full-order $H_{11,706}(j\omega)$ response. The relative errors $|H_{40}(j\omega) - H_{11,706}(j\omega)| / |H_{11,706}(j\omega)|$ are reported in Fig 15.

The Bode plot of the full-order model $H_{11,706}(j\omega)$ took 2,256 seconds versus 4 seconds for the reduced-order model $H_{40}(j\omega)$. Construction of $H_{40}(j\omega)$ took 200 seconds. The Bode plot for the $H_{20}(j\omega)$ only took 1.6 seconds while its construction took 94 seconds. These tests were performed on a SUN UltraSPARC.

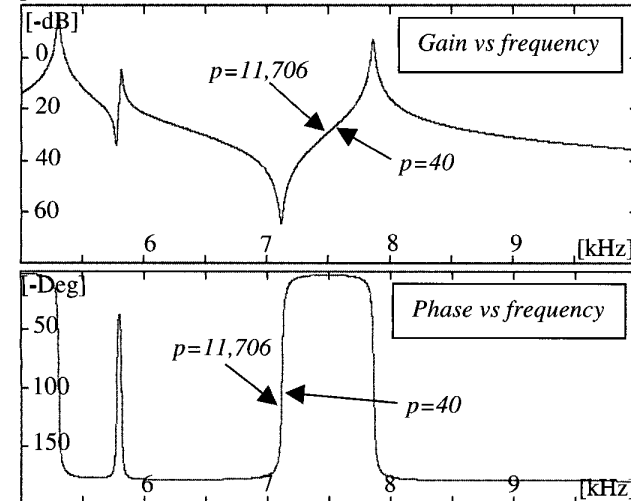


Fig 13-14: Bode and phase of the micromirror in Fig 1, between 5-10 kHz. The response of the reduced-order model is superimposed on the full-order model.

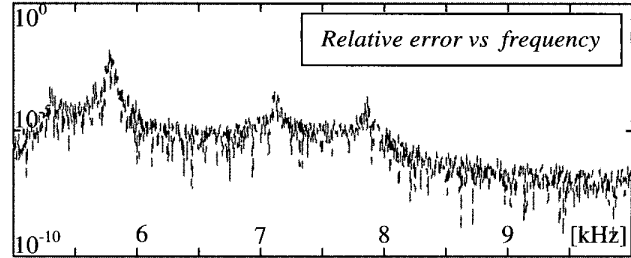


Fig 15: Relative errors of the full-order model and reduced-order between 5-10 kHz.

7 WEB-BASED SUGAR

A Sugar web interface called M&MEMS (Millennium & MEMS) is shown in Fig 16. It allows users to harness the power of UC Berkeley's Millennium cluster to improve simulation performance. Users access the service through a standard web interface. Libraries of mechanical and electrical components will eventually be shared and appended by users. An initial version of the service, available at sugar.millennium.berkeley.edu, came online at the end of August 2001; since that time, 96 users have tried out the service. M&MEMS was also used this semester by graduate students in the local introductory MEMS design course.

There are several advantages to deploying our software as a web service. Once a user has set up an account, she can access her designs and simulations from any machine with a web browser: her desktop, her laptop, perhaps even her cell phone. She will be able to take advantage of software upgrades and fixes as soon as they become available, without having to reinstall the software or download a patch. She is able to take advantage of faster and more sophisticated libraries as they are added to the simulation toolkit, without having to compile and install all the needed components. Ultimately, she will also be able to take advantage of parallelism to run parameter studies quickly, and she will be able to collaborate with other remote M&MEMS users on her designs and simulations.

A M&MEMS client machine only needs a web browser, though a working JVM is useful for viewing deflected structures in 3D. A front-end cluster of three Suns serves web pages to the client, and handles light computational tasks like checking netlist validity. The front-end machines save user information and simulation requests at a dedicated database server node. After a simulation request is entered into the database, it is retrieved by a node in the main cluster (Pentium 3 machines running Linux), where the simulation is run. Upon completion, the node writes simulation results back to the database, where they are available to the client.

As we continue to work to improve the functionality and robustness of M&MEMS, we are also working to integrate the web service with our other research efforts. In particular, we plan to add support for feedback from and comparison to lab measurement data.

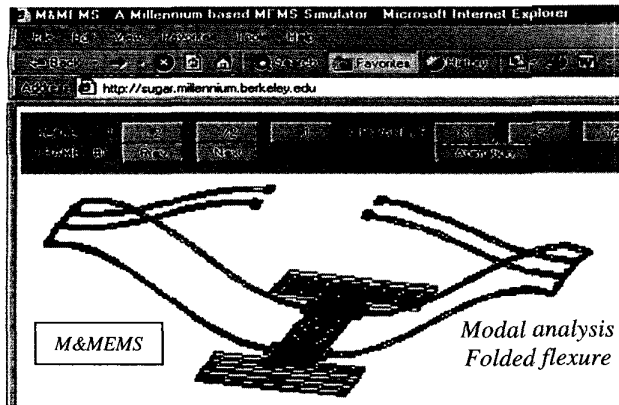


Fig 16: A screen shot of the web-based Sugar simulator. Simulation is performed remotely on the powerful Millennium cluster, reducing software requirement down to just a web browser.

8 FUTURE WORK

Future work will focus on the following aspects of the simulation and synthesis of complex MEMS design. 1) design synthesis and optimization, 2) mechanical modeling extensions, 3) computational advances, 4) user-interface and layout improvements, and 5) sensitivity analysis and validation.

The ultimate goal of Sugar is to serve as a critical tool in the design process for MEMS devices, beginning with a high-level description of the device's desired behavior, design objectives and operating constraints. We propose to integrate our MEMS simulation tools with a MEMS synthesis tool that will assist designers in the early stages of the MEMS design process in addition to providing formal analysis, simulation and parameter optimization at the detailed stage of design. Our initial approach is to incorporate Sugar as a forward simulator into a Multi-Objective Genetic Algorithm (MOGA) to automatically synthesize both the topologies and the sizing of MEMS devices. The MOGA model will include system inputs, the cost function, and the types and numbers of available components such as anchors, beams, electrostatic gaps, combs and springs. As we plan on building up a library of MEMS designs in a Sugar database, case-based reasoning will be used to select a set of starting conceptual designs to form the initial generation of design ideas in the MOGA algorithm [10].

As the micromirror example illustrates, modeling of complex designs can be accomplished with the current use of various types of beams in Sugar. However, there are limitations in relying entirely on this approach. Future work will address this by adding the ability to model thick and thin plates, nonisotropic materials, bi/tri-axial strain, nonlinear damping and contact mechanics. For all of these mechanical extensions, appropriate failure modes (e.g., fatigue, fracture, multi-axial stress limits, buckling, etc.) and design checks will be implemented. Modeling "multiphysics" across several domains is another challenge

and absolutely essential for MEMS devices, which include coupled mechanical, electrical, chemical, thermal, and fluid components.

There are profound implications at the computational level requiring the use of advanced techniques to improve efficiency while balancing accuracy requirements. In future work we will be fully exploiting the use of sparsity, parallelism and reduced order modeling. A related issue is that of how to implement these extensions into a user-friendly environment.

Sensitivity analysis will be used to test the impact of design and process variations on the robustness of the final design. Finally, we intend to integrate Sugar into the entire design process by adding the ability to produce CIF output for fabrication tools and to provide tools to make it easy to compare measured data with our simulations. In summary, we have an ambitious development program, however, the timeline in achieving these advances will depend on future funding levels.

REFERENCES

- [1] Sugar: www-bsac.eecs.Berkeley.edu/~cfm
- [2] J. V. Clark, D. Bindel, N. Zhou, S. Bhave, Z. Bai, J. Demmel, K. S. J. Pister, *Advancements in a 3D Multi-Domain Simulation Package for MEMS*, Proc. of the Microscale Systems: Mechanics and Measurements Symposium, June 4, 2001, Portland OR, USA, pp. 40-45
- [3] J. V. Clark, N. Zhou, D. Bindel, L. Schenato, W. Wu, J. Demmel, K. S. J. Pister, *3D MEMS Simulation Modeling Using Modified Nodal Analysis*, Proceedings of the Microscale Systems: Mechanics and Measurements Symposium, June 8, 2000, Orlando FL, USA pp. 68-75
- [4] Z. Bai, D. Bindel, J. V. Clark, J. Demmel, K. S. J. Pister, N. Zhou, *New Numerical Techniques and Tools in Sugar for 3D MEMS Simulation*, Tech. Proc. of the 4th Intrnl. Conf. on Modeling and Simulation of Microsystems March 19-21, 2001, Hilton Head Island, SC, pp. 31-34
- [5] N. R. Swart, S. F. Bart, M. H. Zaman, M. Mariappan, J. R. Gilbert, and D. Murphy. *AutoMM: Automatic Generation of Dynamic Macromodels for MEMS Devices*. MEMS'98, pp178-183, Heidelberg, Germany
- [6] V. Milanovic, M. Last K.S.J. Pister. *Torsional Micromirrors with Lateral Actuators*. Transducers '01 Eurosensors XV conf, Muenchen, Germany, Jun. 2001
- [7] B. Baidya, S.K. Gupta and T. Mukherjee, *MEMS Component Extraction*, in Intrnl. Conf. on Modeling and Simln. of Micorsystems, San Juan, April 19-21, 1999
- [8] R. Fay, *A new approach to the analysis of the deflection of thin cantilevers*, Journal of Applied Mechanics 28, Trans. ASME, 83, Ser. E, 1961
- [9] M. Abramowitz, A. Stegun, *Handbook of Mathematical Functions*, Dover Publications, Inc, New York, 1972
- [10] N. Zhou, B. Zhu, A. Agogino, K. S. J. Pister, *Evolutionary Synthesis of MEMS Design*. Proceedings of ANNIE 2001, Intell. Eng. Sys. through Artificial Neural Networks, Vol 11, ASME Press, pp. 197-202
- [11] T.-J. Su and R. R. Craig Jr., *Model Reduction and Control of Flexible Structures Using Krylov Vectors*. J. of Guidance. Vol 14, pp. 260-267, 1991